J Eng Math (2009) 65:125–141
DOI 10.1007/s10665-009-9276-0

Diffraction from arbitrarily shaped bodies of revolution: analytical regularization

Sergey B. Panin · Paul D. Smith · Elena D. Vinogradova · Yury A. Tuchkin · Sergey S. Vinogradov

Received: 28 November 2007 / Accepted: 11 February 2009 / Published online: 4 March 2009

Abstract A mathematically rigorous and numerically efficient approach, based on analytical regularization, for solving the scalar wave diffraction problem with a Dirichlet boundary condition imposed on an arbitrarily shaped body of revolution is described. Seeking the solution in an integral-equation formulation, the singular features of its kernel are determined, and the initial equation transformed so that its kernel can be decomposed into a singular canonical part and a regular remainder. An analytical transformation technique is used to reduce the problem equivalently to an infinite system of linear algebraic equations of the second kind. Such system can be effectively solved with any prescribed accuracy by standard numerical methods. The matrix elements of this algebraic system are expressible in the terms of the Fourier coefficients of the remainder. Due to the smoothness of the remainder a robust and efficient technique is obtained to calculate the matrix elements. Numerical investigations of structures, such as the prolate spheroid and bodies obtained by rotation of "*Pascal's Limaçon*" and of the "*Cassini Oval*", exhibit the high accuracy and wide possibilities of the approach.

Keywords Analytical regularization · Body of revolution · Dirichlet problem · Scalar wave diffraction

S. B. Panin · P. D. Smith (✉) · E. D. Vinogradova
Department of Mathematics, Macquarie University, Sydney, NSW 2109, Australia
e-mail: pdsmith@maths.mq.edu.au

S. B. Panin
e-mail: serpanin@maths.mq.edu.au

E. D. Vinogradova
e-mail: evinogra@maths.mq.edu.au

S. B. Panin · Y. A. Tuchkin
Institute for Radiophysics and Electronics of NASU, 12, Acad. Proskura Str., 61085, Kharkov, Ukraine

Y. A. Tuchkin
Gebze Institute of Technology, Gebze, Kocaeli, Turkey
e-mail: yury.tu@gmail.com

S. S. Vinogradov
CSIRO, P.O. Box 76, Epping, Sydney, NSW 1710, Australia
e-mail: sergey.vynogradov@csiro.au

1 Introduction

Scattering of acoustic or electromagnetic waves is of widespread interest. The advent of powerful computing resources has facilitated the numerical simulation of many concrete diffraction problems; the many methods developed and refined have had a significant impact in providing numerical solutions and insight into the important scattering mechanisms.

Exact analytical solutions to diffraction boundary-value problems (BVP) for finite bodies are possible only when the geometry of the problem permits separation of the wave equation [1–3]. For example, Bowman et al. [1] have compiled a comprehensive survey of analytical and numerical results for acoustic and electromagnetic scattering by bodies for which the wave equation is separable. Also, for slender bodies that have a particular geometry, the scattered field may be approximated by asymptotic methods (see for example [4]).

However approaches based on surface-integral equations (including various modifications of the Method of Moments (MoM) approach [5] or Nystrom's method [6]), or based on partial differential equations (viz. finite-difference [7] and finite-element techniques [8]), are the standard present-day choice for addressing the general three-dimensional harmonic scattering problem at low and mid-frequencies for arbitrarily shaped bodies. The surface-integral approach has the advantages of reducing the dimensionality of the problem by one, and of transforming an infinite domain to one with finite boundaries in which the far-field radiation condition is automatically satisfied. The strength of the finite-difference and finite-element techniques consists in that the fill-time of the matrix equation derived by these techniques is substantially smaller than that in MoM; the resulting matrix, though much larger than of the MoM matrix, is highly sparse and can be solved using special algorithms. However, Rosen et al. [9] showed that proper discretization of the surface-integral equations can result in sparse or effectively sparse matrices too.

The surface-integral approach applied to exterior domains fails to provide a unique solution at certain frequencies associated with resonances of the interior region. These spurious resonances do not correspond to a physical situation when solving an exterior problem and yield meaningless peaks in the computed scattering characteristics. A great deal of work has been performed to address this difficulty of non-uniqueness and of the evaluation of singular and hypersingular integrals.

In the case of acoustic scattering from soft bodies, which is considered in this paper, it was shown by Leis [10] and Panich [11] that the difficulty of non-uniqueness can be avoided by employing a suitable linear combination of single- and double-layer potentials; the coupling factor must be chosen to be strictly complex when the wave frequency is real. Another, conceptually simplest, way to avoid non-uniqueness is to employ a Green's function that is different from the free space Green's function and has no real-valued frequency of resonance in the interior region; in this approach a substantive amount of effort is focussed on the construction of such a suitable Green's function; see [12].

The integrals containing the singular integrands encountered in these formulations are often evaluated by numerical techniques currently available; for example, for a weak singularity of $1/R$ type, the methods described in [13,14] are applicable. Also the idea of regularization of the singularity is used; see, for example, [15]. This classical idea in potential theory and acoustics involves the subtraction of a function from the integrand, so that the resultant kernel becomes regular, and then addition of an accurate integration of the function back to the equation. It is necessary to emphasise that this is simply a technical simplification of the kernel numerical integration, without any change of the qualitative property of the equation (such as being of the first kind, for example).

Nevertheless, contemporary methods of simulation of a BVP mostly rely on direct numerical techniques. Their shortcomings are well-known and they originate from the usage of ill-posed first-kind Fredholm equations; such equations are ill-posed in their numerical implementation, and therefore cannot be reliably and efficiently solved numerically [16,17]. This is the main reason why it is highly desirable to transform this equation into a second-kind Fredholm equation, which can be treated by stable and fast-converging computational algorithms that enable us to guarantee any pre-specified accuracy of computations. A transformational technique, which might be called a semi-inversion procedure, is described by Vinogradov et al. [18] for *canonically shaped open shells* (spheres, spheroids, cylinders, etc.).

This semi-inversion procedure is a special case of the analytical regularization method (ARM) applied herein to the acoustic wave-diffraction problem with Dirichlet boundary condition on the surface of an arbitrarily shaped body of revolution (BOR). Posing this BVP in the surface-integral-equation formulation, we obtain the singular expansion of the azimuth-angle Fourier coefficients of the integral kernel corresponding to the surface of revolution. Utilizing this expansion, we may transform the initial integral equation to a form in which the kernel can be split into the sum of the azimuth-angle Fourier coefficients of the Green's function (for Laplace's equation) projected onto a unit sphere, and a remainder term. It is crucial that the first two principal singularities of the kernel of the transformed integral equation coincide with those of the Green's function for the Laplace equation associated with a unit sphere. Thus the remainder term in the kernel of the transformed integral equation is a substantially smoother function. The idea of such a splitting in this specific context seems to have been proposed first by Tuchkin [19,20]. The choice of the aforementioned kernel associated with the unit sphere is dictated by the necessity to reduce the problem to an integral equation for which the Analytical Regularization Method is either already established or can be relatively easily constructed; see [16,17,19,20].

We would emphasise that it is a misconception to view this transform, and the method as a whole, as a variant of some perturbation technique. Indeed the difference between the untransformed kernel and the abovementioned kernel for the unit sphere is neither small nor smooth (actually, the difference contains the singularities arising in both kernels). Moreover, a detailed analysis of the kernel singularities shows that, whilst there is a one-parameter family of possible transforms for which the principal or dominant singularity of each kernel is equal, there is only one unique transform for which the first two principal singularities (dominant and subdominant) are equal. This unique transform provides us with the smoothest reminder. That smoothness gives rise to an algebraic system of second kind which possesses excellent qualities for numerical computation, as explained below.

One may conceive of other possibilities for regularization, for example, usage of the solution of the corresponding static problem for the same body of revolution. This idea is indeed fruitful for canonical shapes, when the solution of the static problem is already known; see [18]. Unfortunately, for arbitrarily shaped obstacles, this idea leads nowhere, because the solution of the corresponding static problem has about the same complexity as the dynamical one.

It may be asked why our starting point is an equation of the first kind, when appropriate second-kind integral equations (as in [10,11]) are available. The answer lies in our desire for numerical efficiency. Unfortunately, the kernel of the relevant equation of second kind is not infinitely smooth: all its derivatives of second order are unbounded, and so any standard quadrature formula for numerical integration will have very slow convergence, with attendant impact on the various numerical methods that might be employed for the solution of the integral equation. The structure of the kernel singularities is rather complicated and efficient integration algorithms need the creation of two-dimensional Gaussian quadrature formulae with rather atypical weights (not representable as a product of one-dimensional weights). Estimates show that the complexity of their creation is considerably more complex than the initial problem itself.

Thus, returning to the above-mentioned transformed equation of the first kind, we see that it is formally similar to the canonical integral equation that arises in the BVP for Laplace's equation with a spherical surface; the first two dominant singularities of the kernels are the same, and the smoothness of the remainder allows us to apply Analytical Regularization Method with an effective numerical implementation.

Without going deeply into the mathematical details, a few words, about the nature of the ill-conditioning of the integral equation of the first kind studied in this paper and why it may be transformed to an equation of the second kind, are in order. From the functional-analytic point of view, the well- or ill-posedness of the integral equation is dependent on precisely how it is posed. If the equation operator is considered as an operator on one space (say, L_2, C^m or H^s, and so on), the equation is necessarily ill-posed; however, if we pose the equation on a pair of functional spaces, say A and B, where, roughly speaking, the space A includes as a dense set all the derivatives of the space B, then the equation so posed will be of the second kind. A choice of spaces, such as the pair of Sobolev spaces H^s and H^{s+1} (for any real-valued s), is suitable for such a theoretical investigation, but not for numerical implementation: the problem is that, due to round-off error, the subtleties of the correct functional spaces are lost and, computer computations should be interpreted as though the problem is posed as an operator on *one* space (such as L_2 or

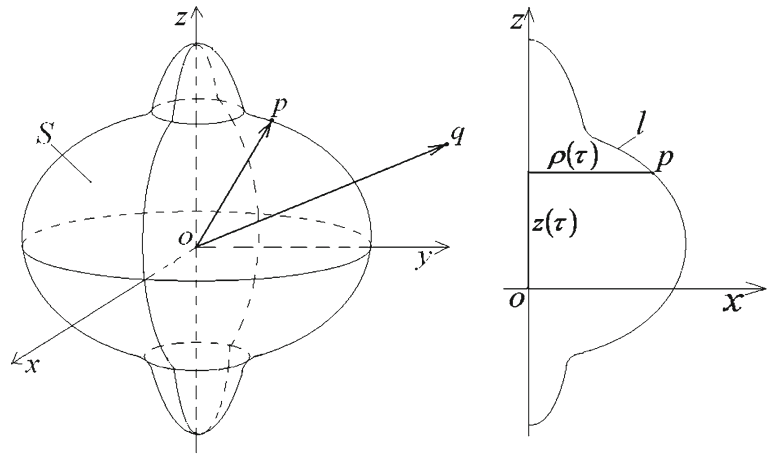

Fig. 1 **a** Surface of revolution; **b** generating curve

L_∞); see [21]. At this informal level of explanation, the Analytical Regularization Method can be understood as a transformation to a suitable functional-analytic setting that can be faithfully reflected in computer calculations. The success of the Analytical Regularization Method in the context of this paper can be attributed, in principle, to the fact that our problem has a well-posed formulation. By contrast, there are "essentially" ill-posed problems for which well-posed formulations are unknown or are too complicated; the Analytical Regularization Method can do nothing to alleviate the ill-posedness of such problems.

Thus, this paper is devoted to the numerical implementation, verification and more detailed development of the Analytical Regularization Method suggested in [19,20]. As mentioned above, non-uniqueness of the solution to the integral equation occurs at a countable set of frequencies at which resonance of the interior region occurs; a suitable alternative choice of Green's function [12] eliminates this difficulty; but for simplicity our exposition will use the standard free-space Green's function, and assume that the corresponding integral equation has a unique solution. A detailed investigation of the elimination of this restriction will be the subject of our next publication.

2 Problem formulation

The geometrical structure of the problem is shown in Fig. 1a. The smooth surface S of the BOR is formed by rotation of a generating curve l around the OZ-axis; see Fig. 1b. Without loss of generality we suppose that l is a plane, smooth and non-self-crossing curve, the ends of which are placed on the OZ-axis. The surface S is supposed to be topologically equivalent to a spherical surface (this excludes surfaces such as a torus or a sphere with multiple handles).

Let the BOR be illuminated by the scalar wave with harmonic temporal dependence

$$U_0(q,\ t) = U^i(q) \exp -(\mathrm{i}\omega t), \tag{1}$$

where ω is angular frequency, and $U^i(q)$ is the velocity potential, which is a given function of observation point $q \in R^3$. We suppose that the function $U^i(q)$ is smooth in some vicinity of S.

We consider the following Dirichlet diffraction problem: find the scattered scalar field $U^s(q)$ which satisfies the Helmholtz equation with the Dirichlet boundary condition

$$(\Delta + k^2)U^s(q) = 0, \quad q \in R^3 \backslash S, \tag{2}$$

$$U^s(q) + U^i(q) = 0, \quad q \in S, \tag{3}$$

where $k = \omega/\upsilon_0$ is the wave number, and υ_0 represents the speed of sound in the medium at the equilibrium state. The Dirichlet boundary condition (3) corresponds to an acoustically soft surface.

For physically reasonable solutions, the Sommerfeld radiation conditions must be imposed. In three-dimensional problems the condition is:

$$r\left(\frac{\partial U^s}{\partial r} - \mathrm{i}kU^s\right) \to 0, \tag{4}$$

uniformly with respect to direction as $r \to \infty$. For smooth closed scatterers, the enforcement of conditions (2)–(4) is adequate to ensure that a unique solution to the scattering problem at hand exists [12,22].

The general solution to the Dirichlet BVP can be expressed in the form of a surface integral [12]:

$$U^s(q) = \int\limits_S \int j(p)G(q,p)\mathrm{d}s_p, \quad q \in R^3, \tag{5}$$

$$G(q,p) = -\frac{1}{4\pi}\frac{\exp(\mathrm{i}kR(q,p))}{R(q,p)}, \tag{6}$$

where $j(p)$ is the unknown single-layer distribution at the surface point p, (actually, $j(p)$ is the normal derivative of the velocity potential along the outward normal to the surface S: $j(p) = \partial U^s(p)/\partial n_p$), $G(q,p)$ is the Green's function for the Helmholtz equation in three-dimensional free space, and $R(q,p) = |q-p|$ is the distance between any two points in space. Applying (3)–(5), we arrive at the following Fredholm integral equation of the first kind:

$$\int\limits_S \int j(p)G(q,p)\mathrm{d}s_p = -U^i(q), \quad q,p \in S, \tag{7}$$

which determines the unknown function $j(p)$. The integrand of (7) has a weak singularity in the sense that the integral operator is compact in $L_2(S)$ space; see [12].

3 Parameterization

Let the generating curve l, placed in the XOZ-plane, have a smooth parameterization,

$$z = z(\tau), \quad \rho = \rho(\tau) \quad \tau \in [0,\pi], \tag{8}$$

where $z = z(\tau)$ and $\rho = \rho(\tau)$ are given functions of the zonal parameter τ, which are cylindrical coordinates of the point $p = p(z,\rho,\varphi = 0) \in l$; see Fig. 1b. The upper and lower end-points ($\rho = 0$) of the contour l correspond to parameter values $\tau = 0$, and $\tau = \pi$ respectively, and $\rho(\tau) > 0$ when $\tau \in (0,\pi)$. The functions are supposed to satisfy the conditions:

$$\text{if} \quad \ell(\tau) = \sqrt{\{z'(\tau)\}^2 + \{\rho'(\tau)\}^2}, \tau \in [0,\pi], \text{then } 0 < \ell(\tau) < \infty, \tag{9a}$$

and

$$z^{(2k+1)}(0) = z^{(2k+1)}(\pi) = 0, \rho^{(2k)}(0) = \rho^{(2k)}(\pi) = 0, \quad k = 0,1,2,\ldots,K, \tag{9b}$$

where the integer K describes the surface smoothness. The condition (9a) applied to an element of arc length $\ell(\tau)$ ensures one-to-one parameterization of the curve l. Also, the following inequalities are imposed by (9a) and (9b):

$$\rho'(0) > 0; \rho'(\pi) < 0. \tag{9c}$$

The conditions (9b) and (9c) mean perpendicularity of the contour l to the OZ-axis in the end-points.

For the parameterization (8), the zonal parameter τ can be chosen to be a normalized arc-length of the curve: $\tau = \tau(p) = \pi s(p)/L$, where $s(p)$ is the arc-length of the point p from an upper end-point, and L is the length of l.

The closed surface of revolution S formed by rotation of the generating curve l around OZ-axis is now described in cylindrical coordinates $\{z,\rho,\varphi\}$ by

$$x = \rho(\tau)\cos\varphi, \quad y = \rho(\tau)\sin\varphi, \quad z = z(\tau), \quad \tau \in [0,\pi], \quad \varphi \in [0,2\pi]. \tag{10}$$

In these coordinates, the surface element $\mathrm{d}s$ for the surface of revolution has the form $\mathrm{d}s = \rho(\tau)\ell(\tau)\mathrm{d}\tau\mathrm{d}\varphi$. Due to axial symmetry of the surface S, the distance $R(q, p)$ is a function of the squared difference of the azimuthal angles $\varphi = \varphi_q - \varphi_p$.

4 Extraction of the kernel singularity

The free-space Green's function for Laplace's equation restricted to a unit sphere has the following Fourier expansion in the spherical coordinates $(r,\ \vartheta,\ \varphi)$:

$$g\left(\vartheta_q, \vartheta_p, \varphi\right) = \sum_{m=0}^{\infty} (2 - \delta_{m0})\, g^m\left(\vartheta_q, \vartheta_p\right)\, \cos m\varphi, \tag{11}$$

where

$$g^m(\vartheta, \tau) = -\frac{1}{4\pi^2}\int_0^{\pi} \frac{\cos m\varphi \mathrm{d}\varphi}{[2(1-\cos\psi)]^{1/2}} = -\frac{1}{4\pi}\sum_{n=|m|}^{\infty} \frac{1}{n+1/2}\hat{P}_n^{|m|}\left(\cos\vartheta_q\right)\hat{P}_n^{|m|}\left(\cos\vartheta_p\right); \tag{12}$$

here δ_{mn} is the Kronecker delta; $\hat{P}_n^m(x) = \sqrt{\left(n+\frac{1}{2}\right)\frac{(n-m)!}{(n+m)!}}\ P_n^m(x)$, where $P_n^m(x)$ is the associated Legendre function of the first kind. Also $g^m(\vartheta, \tau)$ is the Fourier coefficient of the function $g\left(\vartheta_q, \vartheta_p, \varphi\right)$, from which the first equality in (12) is seen to hold with $\cos\psi = \cos\vartheta\cos\tau + \sin\vartheta\sin\tau\cos\varphi$, $\vartheta, \tau \in [0, \pi]$.

The second equality in (12) is derived from a representation for the distance $|q - p|$ between points $q = (r_q, \vartheta_q, \varphi_q)$ and $p = (r_p, \vartheta_p, \varphi_p)$, expressed in the spherical coordinate system (see Chap. 2, Sect. 10, formula (26) of [23]) by

$$|q-p|^{-1} = \sum_{l=0}^{\infty}\sum_{m=-l}^{l} \frac{4\pi}{2l+1}\frac{r_<^l}{r_>^l}Y_{lm}(\vartheta_q, \varphi_q)Y_{lm}(\vartheta_p, \varphi_p),$$

where $r_< = \min(r_q, r_p)$ and $r_> = \max(r_q, r_p)$, together with the well-known addition theorem for spherical harmonics

$$Y_{lm}(\vartheta, \varphi) = (2\pi)^{-1/2}\mathrm{e}^{\mathrm{i}m\varphi}\left[\frac{2l+1}{2}\frac{(l-m)!}{(l+m)!}\right]^{1/2} P_l^m(\theta);$$

substituting and equating the Fourier coefficients in the formula for $|q-p|^{-1}$, when the points p and q lie on the unit sphere, produces the second equality in (12). The expansion for $g^m\left(\vartheta_q, \vartheta_p\right)$ has a diagonal matrix form: it does not involve any terms proportional to $\hat{P}_n^{|m|}(\cos\vartheta_q)\hat{P}_l^{|m|}(\cos\vartheta_p)$ for $n \neq l$.

Introduce the unknown function $X(\tau, \varphi)$ which is proportional to the single-layer distribution on S:

$$X(\tau, \varphi) = -\xi(\tau)\ell(\tau)j(\tau, \varphi), \quad \tau \in [0, \pi], \quad \varphi \in [0,\ 2\pi], \tag{13}$$

where $\xi(\tau) = \sqrt{\rho(\tau)/\sin\tau}$ is a scale function defined correctly for all $\tau \in [0, \pi]$, if one understands the values $\xi(0) = \xi(+0)$, and $\xi(\pi) = \xi(\pi - 0)$ as the corresponding limiting values of $\xi(\tau)$. According to (9b) and (9c) such limits exist and are strictly positive: $0 < \xi(\tau) < \infty$, $\tau \in [0, \pi]$.

Now Eq. 7 becomes

$$\int_{-\pi}^{\pi}\mathrm{d}\varphi_p \int_0^{\pi}\mathrm{d}\tau_p\sqrt{\rho\left(\tau_p\right)\sin\tau_p}X\left(\tau_p, \varphi_p\right)G\left(\tau_q, \tau_p, \varphi_q, \varphi_p\right) = U^i\left(\tau_q, \varphi_q\right), \quad q \in S. \tag{14}$$

Expand in Fourier series all functions $f(x, \varphi)$ of the azimuthal angle that occur in (14) in the form

$$f(\tau, \varphi) = \sum_{m=-\infty}^{\infty} f^m(\tau)\ \mathrm{e}^{\mathrm{i}m\varphi}, \quad f^m(\tau) = \frac{1}{2\pi}\int_{-\pi}^{\pi}\mathrm{d}\varphi\mathrm{e}^{-\mathrm{i}m\varphi}f(\tau, \varphi).$$

Now, due to axial symmetry of the surface S, we can substitute the Fourier expansions of all functions in (14) and perform term-by-term integration in (14) over φ_p (this term-by term integration can be mathematically justified), and then obtain a set of independent integral equations:

$$\int_0^{\pi} \mathrm{d}\tau_p \sqrt{\rho\left(\tau_p\right) \sin\tau_p} G^m\left(\tau_q, \tau_p\right) X^m\left(\tau_p\right) = \frac{1}{2\pi} U^m\left(\tau_q\right), \quad m = 0, \pm 1, \pm 2, \ldots, \quad q \in S, \tag{15}$$

where each equation corresponds to value m of azimuthal index. Thus, Eq. 14 is separated into an infinite set of single integral equations over the zonal parameter τ for determining the azimuthal Fourier coefficients $X^m(\tau, \varphi)$ of the normalized single-layer distribution (13).

The singularities of the azimuthal Fourier coefficients $G^m\left(\tau_q, \tau_p\right)$ of the Green's function in (15) have a rather complicated structure. Their asymptotic expansion shows that when the points q and p are close ($p \to q$ for $p, q \in S$), the function $G^m\left(\tau_q, \tau_p\right)$ exhibits two kinds of singularities: a singularity of form $|q-p|^{-1}$ in the vicinities of the pole-points (when $q \in OZ$), and otherwise a logarithmic one:

$$G^m(\tau, \tau+\delta) = \begin{cases} -\dfrac{1}{4\pi} \dfrac{\exp\left(\mathrm{i}k\ell(\tau)|\delta|\right)}{\ell(\tau)\,|\delta|} \delta_{m0} + K^m(\tau, \delta), & q \in OZ, \\ \dfrac{1}{4\pi^2} \dfrac{1}{\rho(\tau)} \log|\delta| \left\{1 + \sum\limits_{n=1}^{N} A_n^m(\tau)\delta^n\right\} + F_{N+1}^m(\tau,\ \delta), & q \notin OZ, \end{cases} \tag{16}$$

where $\delta = \tau_p - \tau_q$, $|\delta| \ll 1$; $K^m(\tau, \delta)$ and $F_{N+1}^m(\tau, \delta)$ are functions that are smoother in comparison with preceding terms. When $\delta \to 0$, the function $F_{N+1}^m(\tau, \delta)$ exhibits singular behaviour of the form $\delta^{N+1} \log|\delta|$, and the first terms in the series are

$$A_1^m(\tau) = -\frac{\rho'(\tau)}{2\rho(\tau)}, \quad A_2^m(\tau) = \frac{4\left(\left\{\rho'(\tau)\right\}^2 - \rho(\tau)\rho''(\tau)\right) + \left\{\rho'(\tau)\right\}^2 - \left\{z'(\tau)\right\}^2 + 4\left(m^2 - k^2\rho^2(\tau)\right)\ell^2(\tau)}{16\rho^2(\tau)}.$$

Now, on the basis of the singular expansion (16) we introduce the remainder

$$D^m\left(\tau_q, \tau_p\right) = \xi\left(\tau_q\right)\xi\left(\tau_p\right) G^m\left(\tau_q, \tau_p\right) - g^m\left(\tau_q, \tau_p\right), \quad m = 0, \pm 1, \pm 2, \ldots, \quad \text{for } \tau_{q,p} \in [0, \pi], \tag{17}$$

where $g^m(\tau_q, \tau_p)$ is given by the expansion (12), which functionally defines the mth azimuthal Fourier coefficients of the Green's function for Laplace's equation projected onto a unit sphere. The function $D^m\left(\tau_q, \tau_p\right)$ may be shown to have the representation for $|\delta| \ll 1$:

$$D^m(\tau,\ \tau+\delta) = \frac{1}{64\pi^2} \frac{\delta^2 \log|\delta|}{\sqrt{\sin\tau \sin(\tau+\delta)}} \left(\left[4m^2 - 1\right]\left\{\frac{\ell^2(\tau)}{\rho^2(\tau)} - \frac{1}{\sin^2\tau}\right\} - 4k^2\left(\ell^2(\tau) - 1\right)\right) + f_3^m(\tau,\ \delta), \tag{18}$$

where the function $f_3^m(\tau,\ \delta)$ has the same smoothness as $F_3^m(\tau,\ \delta)$, and the expression in curly brackets is finite and smooth in the interval $(0, \pi)$.

It is worth stressing that, as a result of the careful choice of the rescaling factor $\xi\left(\tau_q\right)\xi(\tau_p)$ in (17), the remainder term so introduced does not have either the principal singular term ($\sim \log|\delta|$) or the next subordinate term ($\sim \delta \log|\delta|$) in its expansion (18). The expansion characterises the degree of smoothness of the remainder $D^m\left(\tau_q, \tau_p\right)$; it can be shown that all its first derivatives are continuous, and the second mixed derivative lies in the space $L_2([0, \pi] \times [0, \pi])$ of square integrable functions:

$$\int_0^{\pi}\int_0^{\pi} \mathrm{d}\tau_q \mathrm{d}\tau_p \sin\tau_q \sin\tau_p \left|\frac{\partial^2 D^m\left(\tau_q, \tau_p\right)}{\partial\tau_q \partial\tau_p}\right|^2 < \infty.$$

The behaviour of the remainder, when the observation and integration points coincide, can be expressed as an expansion in terms of the power of the small fixed value φ_0 of the azimuthal parameter, of the form

$$D^m(\tau, \tau) = \frac{1}{4\pi^2} \frac{1}{\sin\tau} \sum_{l=0}^{\infty} B_l^m(\tau)\varphi_0^l + \frac{1}{\pi}\int_{\varphi_0}^{\pi} \mathrm{d}\varphi \cos m\varphi D(\tau, \tau, \varphi), \tag{19}$$

where $\varphi_0 \ll 1$, $D\left(\tau_q, \tau_p, \varphi\right) = \xi\left(\tau_q\right)\xi(\tau_p)G\left(\tau_q, \tau_p, \varphi\right) - g\left(\tau_q, \tau_p, \varphi\right)$ is the smooth function evaluated at $\tau = \tau_q = \tau_p$ on the interval $\varphi \in [\varphi_0, \pi]$, and the first few terms in the series are given by

$$B_0^m(\tau) = \log\left(\frac{\ell(\tau)}{\xi(\tau)}\right), \quad B_1^m(\tau) = -\mathrm{i}k\rho(\tau), \quad B_2^m(\tau) = \frac{1}{4}k\rho(\tau)\left[k\rho(\tau) - 2m\right],$$

$$B_3^m(\tau) = \frac{1}{18}\mathrm{i}k\rho(\tau)\left[3m^2 + k^2\rho^2(\tau) - 3mk\rho(\tau)\right].$$

In what follows we will consider the expansion of the remainder $D^m\left(\tau_q, \tau_p\right)$ in the double Fourier–Legendre series,

$$D^m\left(\tau_q, \tau_p\right) = -\frac{1}{4\pi}\sum_{k=|m|}^{\infty}\sum_{l=|m|}^{\infty} D_{kl}^m \hat{P}_k^{|m|}\left(\cos\tau_q\right)\hat{P}_l^{|m|}\left(\cos\tau_p\right). \tag{20}$$

The decay rate of the coefficients D_{kl}^m is dictated by the properties of the function $D^m(\vartheta, \tau)$ and its derivatives. The connection between the smoothness of a 2π-periodic function $f(t)$ and the decay rate of its Fourier coefficients f_n is well studied (see [24], for example). In particular, if $f(t)$ has m derivatives in a 2π-periodical sense (i.e., $f^{(k)}(-\pi + 0) = f^{(k)}(\pi - 0), k = 0, 1, 2, \ldots, m-1$) and $f^{(m)}(t) \in L_2[-\pi, \pi]$, then the following inequality is valid (see [24]): $\sum_{n=-\infty}^{\infty}(1 + |n|)^{2m}|f_n|^2 < \infty$. Similar results can be expected to hold for Fourier–Legendre series and Fourier–Jacobi series but, to the best of our knowledge, the subject is not well studied, especially for multidimensional series—at least for a function of the type $D^m(\vartheta, \tau)$ which possesses a complex structure of singularities in its mixed derivatives. Thus, in arriving at an estimate for the decay rate, the main task is to construct the singular expansion of $D^m(\vartheta, \tau)$ as explained in [17]. These analytical calculations are bulky and excessively long to reproduce in this paper, but employing this information, it is then possible to show that the matrix elements D_{kl}^m are decreasing sufficiently rapidly, when $k, l \to \infty$, so that the following double series with weighting coefficient $\varsigma_k = (k + 1/2)$ is convergent:

$$\sum_{k=|m|}^{\infty}\sum_{l=|m|}^{\infty}(\varsigma_k\varsigma_l)^2\left|D_{k\,l}^m\right|^2 < \infty.$$

Calculation of the matrix elements D_{kl}^m of the remainder is based on the inverse Fourier–Legendre transformation, leading to the following triple integration:

$$D_{kl}^m = -4\pi\int_0^{\pi}\int_0^{\pi}\mathrm{d}\tau_q\mathrm{d}\tau_p\ \sin\tau_q\sin\tau_p\hat{P}_k^{|m|}\left(\cos\tau_q\right)\hat{P}_l^{|m|}\left(\cos\tau_p\right)D^m\left(\tau_q,\ \tau_p\right), \tag{21a}$$

$$D^m\left(\tau_q, \tau_p\right) = \frac{1}{\pi}\int_0^{\pi}\mathrm{d}\varphi\cos m\varphi D\left(\tau_q, \tau_p, \varphi\right), \tag{21b}$$

where one can observe that $D_{kl}^{-m} = D_{kl}^m$, and $D_{kl}^m = D_{lk}^m$. Using the representation (18), and Kantorovich's method [25] of extraction of the known singularities of an integrand, one can construct a reliable and efficient scheme of numerical integration (21a) of the smooth remainder (21b).

5 Algebraization of the integral equation

Inserting (17) in Eq. 15, and multiplying both sides by $\xi(\tau)$, one obtains:

$$\int_0^{\pi}\mathrm{d}\tau_p\sin\tau_p\left\{g^m\left(\tau_q, \tau_p\right) + D^m\left(\tau_q, \tau_p\right)\right\}X^m(\tau_p) = \frac{\xi\left(\tau_q\right)}{2\pi}U^m\left(\tau_q\right), \quad m = 0, \pm1, \pm2, \ldots, \quad q \in S. \tag{22}$$

Thus the integral equation so obtained has its kernel expressed as a sum of $g^m(\tau_q, \tau_p)$—this term involves all the singularities of the kernel—and the smooth function $D^m(\tau_q, \tau_p)$. This reformulation of the initial problem seems to have been first suggested by Tuchkin [19,20]. Now we expand the right-hand side of (22) in Fourier–Legendre series with known (computable) coefficients,

$$\xi(\tau)U^m(\tau) = -\frac{1}{2}\sum_{n=|m|}^{\infty} u_n^m \hat{P}_n^{|m|}(\cos\tau), \quad u_n^m = -2\int_0^{\pi} \mathrm{d}\tau \sin\tau \hat{P}_n^{|m|}(\cos\tau)\,\xi(\tau)U^m(\tau). \tag{23}$$

Finally, also expanding the function $X^m(\tau)$ via

$$X^m(\tau) = \sum_{n=|m|}^{\infty} x_n^m \hat{P}_n^{|m|}(\cos\tau), \tag{24}$$

we reduce the initial problem to determining the unknown coefficients x_n^m. In accordance with the definition (13), these coefficients are the Fourier–Legendre coefficients of the normalized single-layer distribution. We pose the problem in such way that the sequences $\{x_n^m\}_{n=|m|}^{\infty}$ for $m = 0, \pm1, \pm2, \ldots$ belong to the set of square summable sequences with weights ς_n (i.e., belong to weighted l_2 space):

$$\sum_{n=|m|}^{\infty} \varsigma_n \left|x_n^m\right|^2 < \infty.$$

The motivation for such posing is the following. As is well known (see, for example, Theorem 8 in Subsect. 4.7, p. 208 of [26]), the unknown distribution is infinitely smooth when both the obstacle surface and the field incident on it are infinitely smooth. In this case, the quantity $N_s = \sum_{n=|m|}^{\infty} n^{2s}\left|x_n^m\right|^2 < \infty$ for any arbitrarily large s. On the other hand, if the surface has singularities such as edges and so on, the inequality is valid only for $s \le 1/2$. We suppose that our surface is smooth, so that formally any large s can be specified in the posing of the problem. However, if the (smooth) surface has regions with small radii of curvature, the values N_s for $s > 1/2$ will be large, signalling some physical inadequacy of the posing. The class of solutions with $s = 1/2$ somehow reflects the "most physical" posing of the problem. (Note that we cannot take $s < 1/2$, because that leads again to a different kind of physical inadequacy—infinite energy of the field, and this class does not provide us with the final system of the second kind below.)

Substituting the expansions (12), (20), (23) and (24) in (22) and integrating term-by-term with respect to the zonal parameter τ_p on the whole interval $[0, \pi]$, we obtain the following series equation:

$$\sum_{n=|m|}^{\infty} \varsigma_n^{-1} x_n^m \hat{P}_n^{|m|}(\cos\tau) + \sum_{k=|m|}^{\infty}\sum_{l=|m|}^{\infty} D_{kl}^m x_l^m \hat{P}_k^{|m|}(\cos\tau) = \sum_{n=|m|}^{\infty} u_n^m \hat{P}_n^{|m|}(\cos\tau), \quad \tau \in [0, \pi]. \tag{25}$$

This equation immediately gives us the infinite system of linear algebraic equations for each fixed $m = 0, \pm1, \pm2, \ldots$:

$$\hat{x}_n^m + \sum_{l=|m|}^{\infty} \hat{D}_{nl}^m \hat{x}_l^m = \hat{u}_n^m, \quad n = |m|, |m|+1, |m|+2, \ldots, \tag{26}$$

where we have introduced the following rescaled variables and coefficients:

$$\hat{x}_n^m = \varsigma_n^{-1/2} x_n^m, \quad \hat{D}_{nl}^m = \varsigma_n^{1/2}\varsigma_l^{1/2} D_{nl}^m, \quad \hat{u}_n^m = \varsigma_n^{1/2}\, u_n^m.$$

The previously explained decay rate of the Fourier–Legendre coefficients D_{nl}^m implies that the matrix elements $\hat{D}_{nl}^m$ also decrease sufficiently rapidly, when $k, l \to \infty$, so that the following weighted double series is convergent:

$$\sum_{n=|m|}^{\infty}\sum_{l=|m|}^{\infty} \varsigma_n\varsigma_l \left|\hat{D}_{n\,l}^m\right|^2 < \infty. \tag{27}$$

This is the most important feature of the method constructed herein. Thus the matrix operator of the infinite system (26) is of second kind, being a compact perturbation of the identity operator in a suitable Hilbert space. It would seem that there are many ways of converting (25) to this format, e.g., by multiplying (25) by the factor ς_s, but in fact such a multiplication does not produce the desired format, because the matrix coefficients $\varsigma_s D_{sn}^m \quad (n, s = |m|, |m|+1, \ldots)$ then do not decay so swiftly. In the next two sections we briefly discuss the reasons for the necessity of regularization and the main stages of its implementation.

6 Equations of the first and second kind

Numerical studies of BVP for static fields or wave scattering usually produce finite algebraic systems of the form $\mathbf{A}_N \mathbf{x}^N = \mathbf{b}^N$ with a matrix operator $\mathbf{A}_N$ of dimension N, which is obtained by truncation of a corresponding infinite system of the first kind

$$\mathbf{A}\mathbf{x} = \mathbf{b}, \tag{28}$$

where the unknown $\mathbf{x}$ lies in a given Hilbert space B_1, and the known vector $\mathbf{b}$ belongs to a possibly different Hilbert space B_2. Conceptually, the Eq. 28 may be regarded as an explicit (or implicit) "algebraization" of a first-kind integral equation by some means of projection and discretization. It is known [27,28] that, as truncation number N increases, the solution $\mathbf{x}^N$ of a first kind system generally does not converge to the solution $\mathbf{x}^\infty$ of the untruncated system (28) in any metric, or if it does, the condition number $\nu(N)$ of the matrices $\mathbf{A}_N$ increase unboundedly: $\nu(N) \to \infty$ when $N \to \infty$. The solution accuracy degrades, as N increases, to the point where the computed solution contains no significant digits. However, the residual $\chi(N) = \mathbf{A}^N \mathbf{x}^N - \mathbf{b}^N$ may be deceptively small (see [21]), and other more indirect measures, such as energy balance, may be equally misleading; the only sure way to assess accuracy—or detect numerical catastrophe—is by direct calculation of $\nu(N)$.

On the other hand, suppose that the initial BVP is transformed to an infinite system of algebraic equations of the second kind in l_2,

$$(\mathbf{I} + \mathbf{H})\,\hat{\mathbf{x}} = \hat{\mathbf{b}}, \tag{30}$$

where $\mathbf{I}$ is the identity operator, and $\mathbf{H}$ is a compact operator (in l_2). If it is well posed, the initial BVP possesses a unique solution, and the operator $\mathbf{I} + \mathbf{H}$ is bounded (in l_2) and invertible, and

$$\nu_\infty = \|\mathbf{I} + \mathbf{H}\|_{l_2} \left\| (\mathbf{I} + \mathbf{H})^{-1} \right\|_{l_2} \tag{31}$$

is finite. Due to the compactness of $\mathbf{H}$, a sequence of finite-dimensional matrix operators $\mathbf{H}_N$ may be selected such that $\|\mathbf{H} - \mathbf{H}_N\|_{l_2} \to 0$ and the condition number of the truncated system (30) obeys

$$\nu(N) = \left\| (\mathbf{I} + \mathbf{H})_N \right\|_2 \left\| (\mathbf{I} + \mathbf{H})_N^{-1} \right\|_2 \to \nu_\infty, \quad \text{when } N \to \infty, \tag{32}$$

i.e., it is uniformly bounded for large N. In all practical situations we have examined, such an equation of the second kind is free from the disadvantages described above for a first kind equation.

7 Analytical regularization

The transformation of the operator equation of the first kind into one of the second kind can be implemented on the basis of the ARM, a theoretical scheme that is rather well known in functional analysis; see Krein [29]. Nevertheless, from a practical point of view, its construction is a challenging problem and cannot in general be explicitly obtained.

Implementations of ARM (see, for example [16–20,30,31]) are constructed, as a rule, on the basis of the solution to some relatively simple so-called *canonical problems* [18], which also have the form of integral (or integrodifferential) equations of the first kind

$$\mathbf{W}\mathbf{y} = \mathbf{b}^w, \tag{33}$$

where the solution $\mathbf{y}$ is sought in the space B_1, and the vector $\mathbf{b}^w$ lies in B_2.

In general, the operator $\mathbf{W}$ can be decomposed as a sum $\mathbf{W} = \mathbf{W}_P + \mathbf{W}_S$ of principal ($\mathbf{W}_P$) and subordinate ($\mathbf{W}_S$) parts that correspond to the singular and regular (or at least less singular) part of the operator $\mathbf{W}$. In the simplest case, an effective scheme can be found for inverting $\mathbf{W}_P$, and (33) becomes

$$\left(\mathbf{I} + \mathbf{W}_P^{-1}\mathbf{W}_S\right)\mathbf{y} = \mathbf{W}_P^{-1}\mathbf{b}^w.$$

If the operator $\mathbf{W}_P^{-1}\mathbf{W}_S$ is compact, regularization has been achieved. This transformation, which may be called "semi-inversion," is applicable for "canonical" problems, when the obstacle surface coincides with part of a coordinate surface in a system in which the Helmholtz or Maxwell equations admit variable separation. Examples of this semi-inversion transformation can be found in Shestopalov et al. [17] and Vinogradov et al. [18].

However, in the more general case we introduce a pair of operators $\mathbf{M}_L, \mathbf{M}_R$ generating a multiplicative splitting of $\mathbf{W}_P$ so that $\mathbf{M}_L\mathbf{W}_P\mathbf{M}_R = \mathbf{I}$, and $\mathbf{H}^w = \mathbf{M}_L\mathbf{W}_S\mathbf{M}_R$ is compact. In this case the pair $\mathbf{M}_L, \mathbf{M}_R$ forms a two-sided regularizator.

If the operator $\mathbf{W}_P$ is strongly positive, its inverse $\mathbf{M} = \mathbf{W}_P^{-1}$ exists and a common multiplicative splitting uses the fractional powers: $\mathbf{M}_L = \mathbf{M}^\alpha$, $\mathbf{M}_R = \mathbf{M}^{1-\alpha}$, for some parameter α. Thus one arrives at the equation

$$[\mathbf{I} + \mathbf{H}^w(\alpha)]\mathbf{z} = \mathbf{b}_\alpha^w, \tag{34}$$

where $\mathbf{y} = \mathbf{M}^{1-\alpha}\mathbf{z}$, and $\mathbf{b}_\alpha^w = \mathbf{M}^\alpha\mathbf{b}$. Fortunately for canonical problems the operator $\mathbf{M} = \mathbf{W}_P^{-1}$ can be almost always be adjusted to be a diagonal, positive (and equally singular) operator, that allows us to determine correctly and easily calculate its powers ($\mathbf{M}^{1-\alpha}$ or $\mathbf{M}^\alpha$).

From a numerical point of view the best choice of α is that providing the fastest convergence of truncation method applied to (34). Typically the best choice is $\alpha = 1/2$, for canonical problems arising in potential and diffraction theory [17,19].

Returning to the original problem (28), we are to find a pair of adjusting operators $(\mathbf{K}_L, \mathbf{K}_R)$ to transform the operator $\mathbf{A}$ to an operator $\mathbf{W}$ of some known canonical problem (34):

$$\mathbf{K}_L\mathbf{A}\mathbf{K}_R = \mathbf{W} = \mathbf{W}_P + \mathbf{W}_S.$$

Recalling that the initial BVP is reducible to an integral (or integrodifferential) equation with singular kernel over the obstacle surface, investigation of the kernel behaviour and its *singular expansion* produces a guide to the choice of adjusting operators that should be taken. Although the singular expansion, and the choice of the adjusting operators $\mathbf{K}_L, \mathbf{K}_R$ is not unique, their actual choice is important because it predetermines the smoothness of the operator $\mathbf{H}^w(\alpha) = \mathbf{M}^\alpha\mathbf{W}_S\mathbf{M}^{1-\alpha}$; the smoother the choice of $\mathbf{W}_S$, the better are the properties of $\mathbf{H}^w(\alpha)$.

With these introduced operators, Eq. 28 is thus transformed to the desired equation of the second kind (30), where

$$\mathbf{H} = \mathbf{M}_L\left(\mathbf{K}_L\mathbf{A}\mathbf{K}_R - \mathbf{W}_P\right)\mathbf{M}_R, \quad \mathbf{x} = \mathbf{K}_R\mathbf{M}_R\hat{\mathbf{x}}, \quad \hat{\mathbf{b}} = \mathbf{M}_L\mathbf{K}_L\mathbf{b}.$$

When supplemented with a procedure associated with Abel's integral transform described by Vinogradov et al. [18], the ARM described above produces a robust basis for solving a wide class of static and diffraction problems for open screens of revolution.

The various stages of the ARM can be recognized in the diffraction problem of this paper. Equation (15) corresponds to (28), where the integral operator $\mathbf{A}$ of the first kind is given by $[\mathbf{A}\ f](\tau_p) = -\int_0^\pi \mathrm{d}\tau_p G^m\left(\tau_q, \tau_p\right)\rho(\tau_p)\ell(\tau_p)f(\tau_p)$; $\mathbf{x}$ is the m-th azimuthal Fourier harmonic $j^m\left(\tau_p\right)$ of the single-layer distribution $j(\tau_p)$, and $\mathbf{b} = U^m\left(\tau_q\right)/2\pi$. The singular expansion (16) guides the choice of the adjusting operators as the following multiplication operators:

$$[\mathbf{K}_L f]\left(\tau_q\right) = \xi\left(\tau_q\right) f\left(\tau_q\right); \quad [\mathbf{K}_R f](\tau_p) = \left\{\xi(\tau_p)\ell(\tau_p)\right\}^{-1} f(\tau_p);$$

they transform Eq. 28 to the form (22), which is equivalent to the operator equation (33) for canonical problem, where

$$[(\mathbf{W}_P + \mathbf{W}_S)\ f](\tau_p) = \int_0^\pi \mathrm{d}\tau_p \sin\tau_p \left\{g^m\left(\tau_q, \tau_p\right) + D^m\left(\tau_q, \tau_p\right)\right\} f(\tau_p),$$

$\mathbf{y} = (\mathbf{K}_R)^{-1}\mathbf{x} = -\xi(\tau_p)\ell(\tau_p)j^m(\tau_p) = X^m(\tau_p)$, and $\mathbf{b}^w = \mathbf{K}_L\mathbf{b} = \xi\left(\tau_q\right)U^m\left(\tau_q\right)/2\pi$.

Note that the pair of adjusting operators introduced above gives the best smoothness properties to the subordinate operator $\mathbf{W}_S$. Using the Fourier–Legendre transformation, Eq. 22 is rewritten in the following algebraic form:

$$\varsigma_s^{-1}x_s^m + \sum_{l=|m|}^{\infty} D_{sl}^m x_l^m = u_s^m, \tag{35}$$

in which the diagonal operator $\mathbf{W}_P = \text{diag}\left\{\varsigma_s^{-1}\right\}_{s=|m|}^{\infty}$ is strongly positive, corresponding to the canonical problem for the unit sphere, $\mathbf{W}_S = \left\{D_{sl}^m\right\}_{s,l=|m|}^{\infty}$ is the operator defined by the matrix of the remainder D_{sl}^m, $\mathbf{y} = \left\{x_s^m\right\}_{s=|m|}^{\infty}$, and $\mathbf{b}^w = \left\{u_s^m\right\}_{s=|m|}^{\infty}$.

Equation (35) seems to be reducible to the desired second kind form (30) by simply multiplying by the factor ς_s; but the operator $\left\{\varsigma_s D_{sl}^m\right\}_{s,l=|m|}^{\infty}$ constructed in this way would not have elements that are decaying as most swiftly as possible. Instead we introduce the inverse operator $\mathbf{M} = (\mathbf{W}_P)^{-1}$, and then the multiplicative splitting: $\mathbf{M}_L = \mathbf{M}_R = (\mathbf{M})^{1/2}$.

Thus one arrives at the algebraic system (26), which is equivalent to the operator equation (30), where we have the following notations: $\mathbf{H} = \left\{\hat{D}_{sl}^m\right\}_{s,l=|m|}^{\infty}$, $\hat{\mathbf{x}} = \left\{\hat{x}_s^m\right\}_{s=|m|}^{\infty}$, and $\hat{\mathbf{b}} = \left\{\hat{u}_s^m\right\}_{s=|m|}^{\infty}$. Due to the property (27), the operator $\mathbf{H}$ is not only compact in l_2 space, but is "better" than a Hilbert–Schmidt operator, and in fact belongs to the class of trace operators. Therefore the system (26) is efficiently solvable numerically by means of a truncation procedure with, in principle, any desired accuracy.

8 Numerical results

The numerical implementation of our approach was validated by comparison against the results obtained for canonical geometry structures using the benchmark solutions published in [1,18]. The accuracy and possibilities of this approach may be demonstrated by three examples; the prolate spheroid and the two non-canonical geometrical surfaces obtained by the rotation of "*Pascal's Limaçon*", and the "*Cassini Oval*"; see Fig. 2. They have the generating radius $r(\tau)$, $\tau \in [0, \pi]$ in polar coordinates (where $\rho(\tau) = r(\tau)\sin\tau$, $z(\tau) = r(\tau)\cos\tau$),

$$r(\tau)|_{\text{Ellipse}} = \frac{ab}{\sqrt{a^2\sin^2\tau + b^2\cos^2\tau}}, \quad a > b;$$

$$r(\tau)|_{\text{Limaçon}} = c + b\cos(\tau - \pi), \quad c > b, \quad b + c = 1;$$

$$r(\tau)|_{\text{Oval}} = b\sqrt{\cos 2\tau + \sqrt{\left(\frac{a}{b}\right)^4 - \sin^2 2\tau}}, \quad a > b,$$

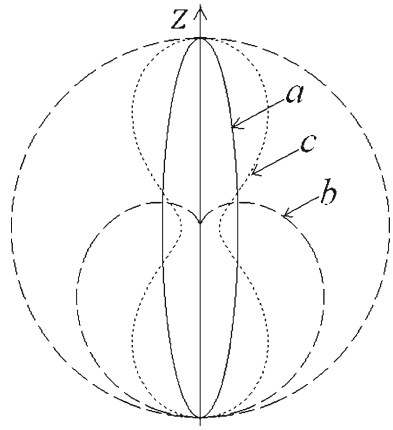

Fig. 2 Cross-sections of the BOR: *Ellipse* (**a**), "*Pascal's Limaçon*" (**b**), and "*Cassini Oval*" (**c**)

where the parameters a, b, and c are given positive constants, and the polar angle τ is equivalent to the zonal parameter. In what follows we will consider the case $m = 0$, which corresponds to axial symmetrical excitation by the plane acoustic wave propagating in the direction of the OZ-axis: $U^i(z) = u_0 \exp(\mathrm{i}kz)$. For definiteness' sake, it is also supposed that $u_0 = 1$, and $a = 1$.

Recall that in the far field region, i.e., at large distance from scattering objects, the scattered velocity potential takes the form [22]

$$U^s(r, \theta, \varphi) = \frac{\exp(\mathrm{i}kr)}{r} F(\theta, \varphi) + O\left(r^{-2}\right),$$

where $F(\theta, \varphi)$ is the so-called scattering pattern, and $\{r, \theta, \varphi\}$ are the spherical coordinates of the observation point. The bistatic cross-section, measuring the energy scattered in the direction determined by $\{\theta, \varphi\}$, is $\sigma(\theta, \varphi) = 4\pi |F(\theta, \varphi)|^2$. The scattering effectiveness in the direction from which the incident wave comes can be defined by the normalized monostatic sonar cross section $\tilde{\sigma} = \sigma/\Omega$, where σ and Ω are respectively the bistatic cross-section and the geometrical cross-section area of the scatterer in the opposite direction of the incident wave.

For the case of axially symmetrical excitation ($m = 0$) of the BOR one can obtain the following expression for the scattering pattern:

$$F(\theta) = -\frac{1}{2} \int_0^{\pi} \mathrm{d}\tau \sqrt{\rho(\tau) \sin\tau}\, J_0(k\rho(\tau) \sin\theta)\, \mathrm{e}^{-\mathrm{i}kz(\tau)\cos\theta} \sum_{n=0}^{\infty} x_n^0 \hat{P}_n(\cos\tau),$$

where J_0 is the Bessel function of the first kind.

The rate of convergence of the system solution as a function of truncation number N may be evaluated, according to Hsaio and Kleinman [32], by the following estimates of error in the maximum norm sense and the relative error:

$$E(N) = \log_{10}\left(\frac{\max\limits_{n \le N} \left|\hat{x}_n^{N+1} - \hat{x}_n^N\right|}{\max\limits_{n \le N_{tr}} \left|\hat{x}_n^N\right|}\right), \quad M(N) = \log_{10}\left(\frac{\left\|\left\{\hat{x}_n^{N+1}\right\}_{n=0}^N - \left\{\hat{x}_n^N\right\}_{n=0}^N\right\|}{\left\|\left\{\hat{x}_n^N\right\}_{n=0}^N\right\|}\right),$$

where the vector $\left\{\hat{x}_n^{N+1}\right\}_{n=0}^N$ denotes the solution of the system (26) truncated to $N + 1$ equations for the case $m = 0$, and $\left\|\left\{\hat{x}_n^{N+1}\right\}_{n=0}^N\right\|$ is its Euclidean norm. Also, the accuracy of the proposed method can be assessed by the discrepancy function

$$\chi(\tau) = \left.\frac{\left|U^s(\tau) + U^i(\tau)\right|}{\left|U^i(\tau)\right|}\right|_S,$$

which measures the degree to which the boundary condition is satisfied on the surface S.

Figure 3a presents the frequency dependence of normalized monostatic sonar cross-section $\tilde{\sigma}$ for prolate spheroids of various aspect ratios b/a as a function of normalized wave number $\tilde{k} = ka\left(\omega = \tilde{k}v_0/a\right)$. In the long-wave regime $\left(\tilde{k} < 1\right)$, the backscattering behaviour substantially depends on the ratio of the spheroid axes: the more prolate spheroid has greater backscattering in comparison with the spheroid of the same geometrical cross-section due to the essential contribution of "nonspecular" diffraction in this frequency domain. For $\tilde{k} > 4$, the normalized sonar cross-section $\tilde{\sigma}$ has approximately the same level for all spheroids under consideration.

The behaviour of the modulus of the single-layer distribution j along the generating curve of the prolate spheroid as a function of the normalized zonal parameter $\tilde{\tau} = \tau/\pi$ is presented in the Fig. 3b. The distribution exhibits maxima on the poles ($\tilde{\tau} = 0,\ \tilde{\tau} = 1$) of the spheroid, and does not have much variation on the interval $\tilde{\tau} \in (0,\ 1)$. In the long-wave regime the single-layer distribution is close to the distribution of charge density in the corresponding electrostatic problem; the level of the maximum at the illuminated pole point ($\tilde{\tau} = 1$) grows with frequency.

As we can see in Fig. 4a, the normalized sonar cross-sections for the BOR of "*Pascal's Limaçon*" for different parameters differ little in behaviour and in level; as a whole the backscattering is quite similar to that for a sphere. On the illuminated side ($\tilde{\tau} = 1$) the modulus of the single-layer distribution has a maximum growing with the

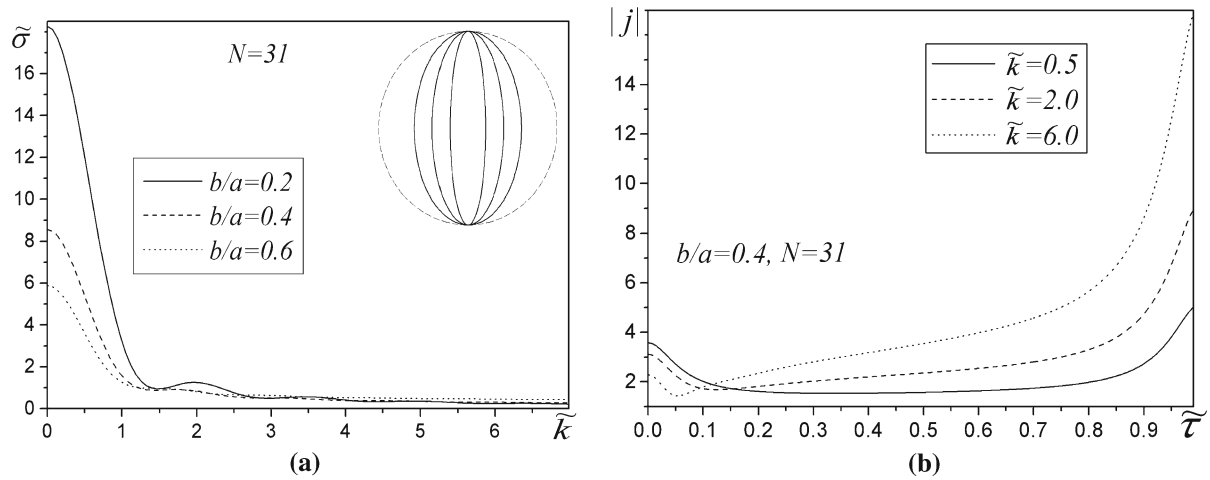

Fig. 3 **a** Normalized sonar cross-section $\tilde{\sigma}$ as a function of normalized wave number $\tilde{k}$ for the prolate spheroid; **b** Modulus of the single-layer distribution j versus the normalized zonal parameter $\tilde{\tau}$

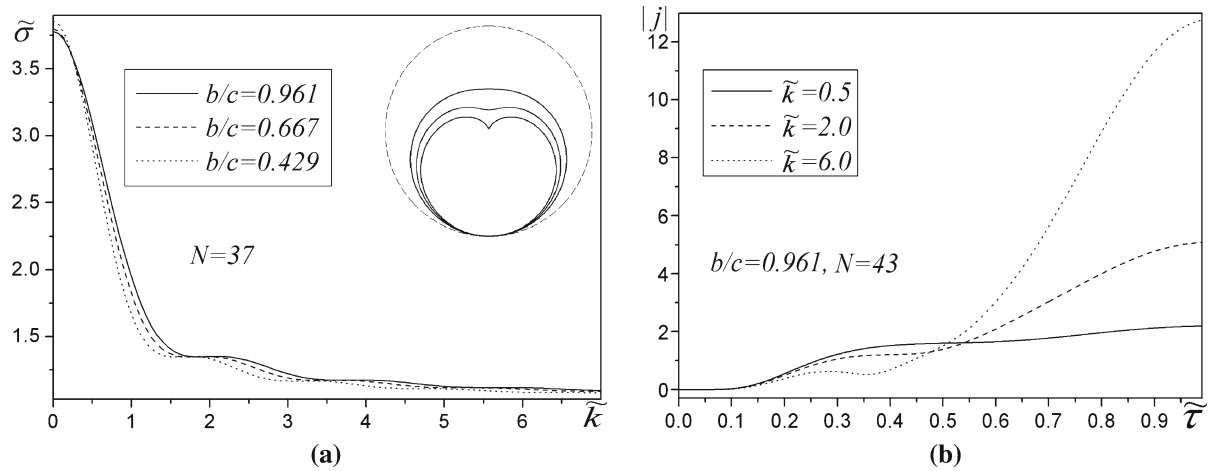

Fig. 4 **a** Normalized sonar cross-section $\tilde{\sigma}$ as a function of normalized wave number $\tilde{k}$ for the BOR of "*Pascal's Limaçon*"; **b** Modulus of the single-layer distribution j versus the normalized zonal parameter $\tilde{\tau}$

frequency of the exciting wave; see Fig. 4b. The minimum value of the single-layer distribution, observed at $\tilde{\tau} = 0$, does not depend much on frequency because of the pronounced geometrical concavity of the BOR in vicinity of $\tilde{\tau} = 0$, for the chosen ratio $b/c = 0.961$.

For the body obtained by rotation of the "*Cassini Oval*", the dependence $\tilde{\sigma}$ has some oscillatory variation as a function of normalized wave number $\tilde{k}$; see Fig. 5a. These variations of backscattering are caused by diffraction from the "wavelike" flank side of the body. The modulus of the single-layer distribution, shown in Fig. 5b, exhibits variations as a function of $\tilde{\tau}$ which are also affected by the specific shape of this body.

The range of values of the discrepancy $\chi(\tilde{\tau})$ along the generating curve (as a function of $\tilde{\tau}$) for all bodies considered is of the order of 10^{-3}; see Fig. 6a. Such accuracy, obtained on the body surface itself where the field convergence is worst, confirms the high reliability of the method proposed. The discrepancy for the prolate spheroid has maxima in the vicinity of $\tilde{\tau} = 0$, $\tilde{\tau} = 1$ where there is geometrical narrowing. The discrepancy maxima of the branch for the BOR of the "*Cassini Oval*" occur in the regions where the single-layer distribution rapidly varies; see Fig. 5b.

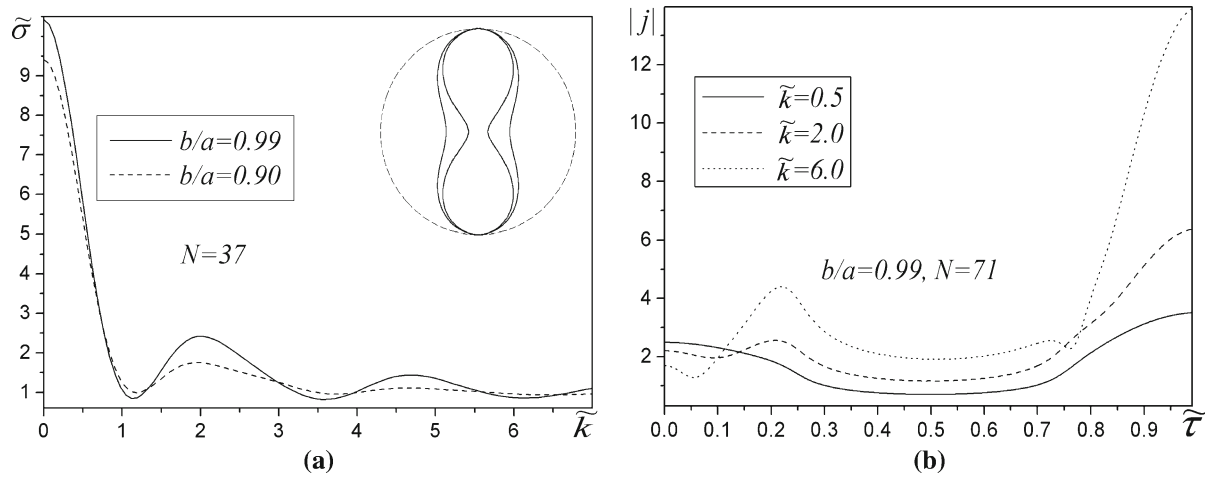

Fig. 5 **a** Normalized sonar cross-section $\tilde{\sigma}$ as a function of the normalized wave number $\tilde{k}$ for the BOR of the "*Cassini Oval*"; **b** Modulus of the single-layer distribution j versus the normalized zonal parameter $\tilde{\tau}$

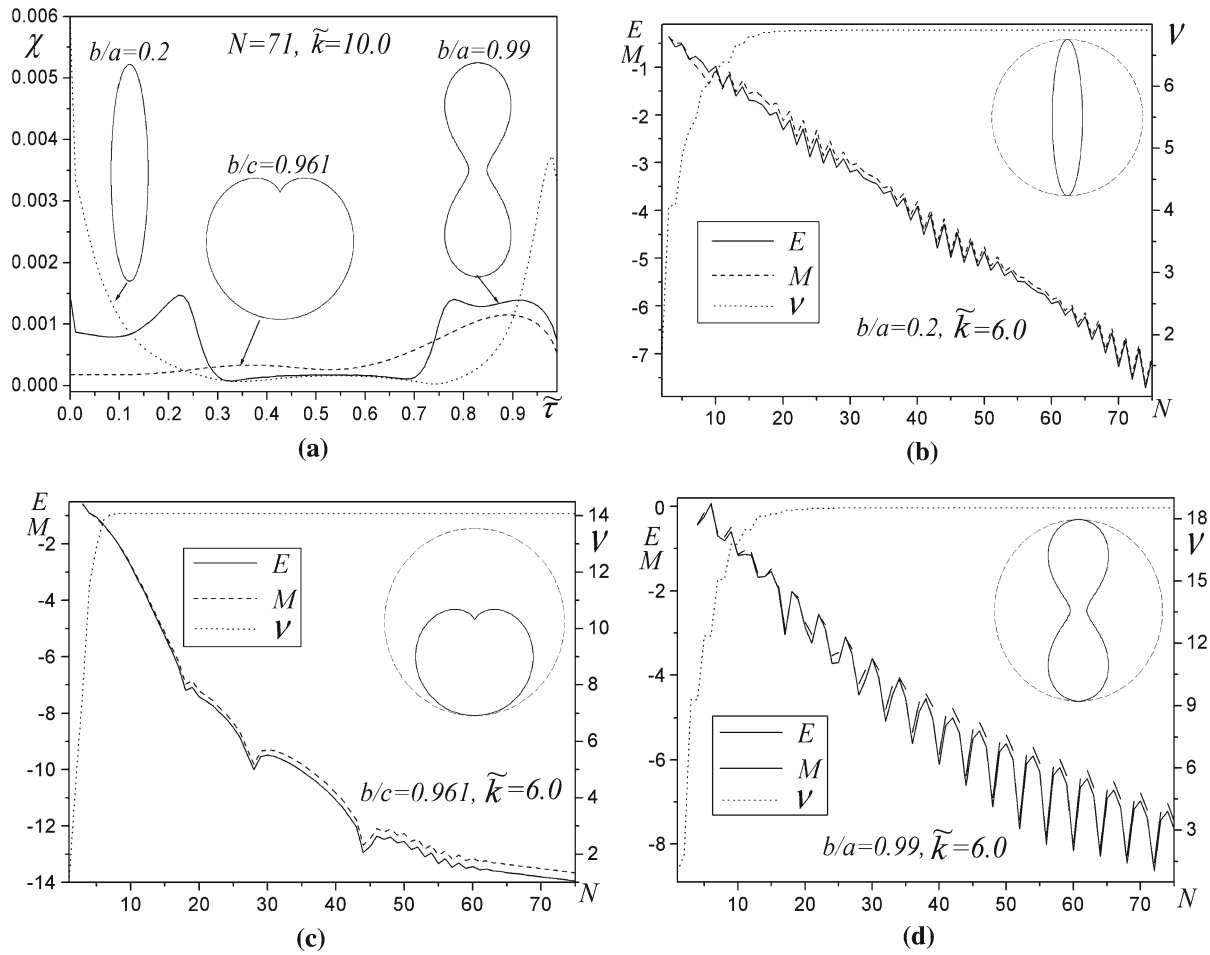

Fig. 6 **a** Discrepancy χ as a function of $\tilde{\tau}$ for bodies of different shapes; error functions E, M, and condition number ν versus N for the prolate spheroid **b**, the BOR of "*Pascal's Limaçon*" **c**, and the BOR of "*Cassini Oval*" **d**

The accuracy of calculation, for various levels of truncation number N, is exemplified by the error functions $E(N)$, $M(N)$ shown in Fig. 6b–d (left vertical axis) for the bodies under consideration. The error functions subside very rapidly for all the body shapes, and have negligible value at about $N = 50$. From this behaviour one can conclude that the calculation process has swift convergence, and high accuracy of the system solution calculation is achievable at rather small truncation numbers. As can be seen from appropriate spherical harmonic expansions, the rate of convergence naturally depends on the geometrical difference between the BOR and a sphere. Our numerical experiments show that the more prolate bodies require larger truncation numbers (for comparable accuracy).

The behaviour of the condition number ν of the truncated matrix of the system (26), which describes the operator of the diffraction problem, as a function of truncation number N, is shown in Fig. 6b–d (right vertical axis) for all the bodies. A very low limiting value of condition number is observed for all bodies considered. This behaviour is the principal advantage of the obtained system of the second kind; it allows us to obtain a stable efficient solution with prescribed accuracy.

9 Conclusion

A new method for solving the scalar Dirichlet diffraction problem, based on the analytical regularization method, is described and implemented for the class of closed smooth scatterers that are arbitrarily shaped bodies of revolution. The proposed approach has a rigorous mathematical basis and can be implemented in a numerically efficient way. Although it can be abstractly described in operator terms, this paper succeeds in making the regularization procedure explicit and computable.

Seeking the solution in the surface-integral-equation formulation, the singularities of the azimuthal angle Fourier coefficients of the integral kernel were investigated. After modifying the integral equation, its kernel was separated into a singular part, which corresponds to the Green's function (for Laplace's equation) projected onto a unit sphere, and a remainder that is a rather smooth function. The solution is obtained in the form of an infinite system of linear algebraic equations of the second kind, which can be solved numerically by means of the truncation method with, in principle, any desired accuracy. The matrix coefficients of this algebraic system are expressible in the terms of the Fourier coefficients of the kernel remainder. The smoothness of the remainder permits a robust and efficient technique to calculate the matrix elements.

This approach was validated by comparison with solutions for bodies of canonical geometry and with other benchmarks. Our investigations of various non-canonical bodies of revolution have shown the capabilities of the approach for practical calculation of the single-layer distribution and far field scattering patterns.

By incorporating the procedure associated with the Abel integral transformation described in Vinogradov et al. [18], this approach may be extended to solve scalar and vector (electromagnetic) diffraction problems for open arbitrary shaped screens of revolution. This will be addressed in future publications.

References

1. Bowman JJ, Senior TBA, Uslenghi PLE (1987) Electromagnetic and acoustic scattering by simple shapes. Hemisphere Pub. Corp., New York
2. Morse PM, Feshbach H (1953) Methods of theoretical physics. McGraw-Hill, New York
3. Stakgold I (1967) Boundary value problems in mathematical physics. Macmillan, New York
4. Van Nhieu MT (1988) A singular perturbation problem: scattering by a slender body. J Acoust Soc Am 83(1):68–73
5. Harrington RF (1968) Field computation by moment methods. Macmillan, New York
6. Atkinson KE (1997) The numerical solution of integral equations of the second kind. Cambridge University Press, Cambridge
7. Hildebrand FB (1968) Finite-difference equations and simulations. Prentice-Hall, Englewood Cliffs, NJ
8. Reddy JN (1993) An introduction to the finite-element method. McGraw-Hill, New York
9. Rosen EM, Canning FX, Couchman LS (1995) A sparse integral equation method for acoustic scattering. J Acoust Soc Am 98(1):599–610
10. Leis R (1965) Zur Dirichletschen randwertaufgabe des auβenraumes der schwingungsgleichung. Mathematische Zeitschrift 90:205–211

11. Panich OI (1965) On the question of the solvability of the exterior boundary problem for the wave equation and Maxwell's equation (in Russian). Usp Mat Nauk 20:205–211
12. Colton D, Kress R (1983) Integral equation methods in scattering theory. Wiley, New York
13. Lachat JC, Watson JO (1976) Effective numerical treatment of boundary integral equations: a formulation for three-dimensional elastostatics. Int J Numer Methods Eng 10:991–1005
14. Seybert AF, Soenarko B, Rizzo FJ, Shippy DJ (1985) An advanced computational method for radiation and scattering for acoustic waves in three dimensions. J Acoust Soc Am 77:362–368
15. Yang S (1997) Acoustic scattering by a hard or soft body across a wide frequency range by the Helmholtz integral equation method. J Acoust Soc Am 102(5):2511–2520
16. Poyedinchuk AYe, Tuchkin YuA, Shestopalov VP (2000) New numerical-analytical methods in diffraction theory. Math Comput Model 32:1026–1046
17. Shestopalov VP, Tuchkin YuA, Poyedinchuk AYe, Sirenko YuK (1997) Novel methods for solving direct and inverse problems of diffraction theory, vol 1: analytical regularization of electromagnetic boundary value problems (in Russian). Publishing House, Kharkov, Osnova
18. Vinogradov SS, Smith PD, Vinogradova ED (2002) Canonical problems in scattering and potential theory, parts I, II. Chapman & Hall/CRC, Boca Raton, FL
19. Tuchkin YuA (2006) Method of analytical regularization: state of art and new approaches. In: IV-th international workshop on electromagnetic wave scattering, vol 2, Gebze, Turkey, pp 43–49
20. Tuchkin YuA (2002) Analytical regularization method for wave diffraction by bowl-shaped screen of revolution. In: Smith PD, Cloude SR (eds) Ultra-wideband, short-pulse electromagnetics, vol 5. Kluwer/Plenum Publishers, New York, pp 153–157
21. Wilkinson JH (1988) The algebraic eigenvalue problem. Oxford University Press, USA
22. Jones DS (1989) Acoustic and electromagnetic waves. Oxford University Press, USA
23. Nikiforov AF, Uvarov VB (1988) Specialnyje funktsii matematicheskoy fiziki. Nauka Publishing House, Moscow. English translation: Nikiforov AF, Uvarov VB (1978) Special functions of mathematical physics. Birkhauser, Boston
24. Shilov GE (1965) Mathematical analysis. Elsevier, New York
25. Salvadori MG, Baron ML (1961) Numerical methods in engineering. Prentice-Hall, New Jersey
26. Bers L, John F, Schechter M (1964) Partial differential equations. Wiley, New York
27. Kantorovich LV, Akilov GP (1964) Functional analysis in normal spaces. Pergamon Press, New York
28. Mittra R, Lee SW (1971) Analytical techniques in the theory of guided waves. The Macmillan Company, New York
29. Krein SG (1982) Linear equations in banach spaces. Birkhauser, Boston
30. Tuchkin YuA (1993) New method in wave diffraction theory by thin screens. Electromagnetics 13:319–338
31. Panin SB, Smith PD, Poyedinchuk AYe (2007) Elliptical to linear polarization transformation by a grating on a chiral medium. J Electromagn Waves Appl 21:1885–1899
32. Hsaio GC, Kleinman RE (1997) Mathematical foundations for error estimation in numerical solutions of integral equations in electromagnetics. IEEE Trans Antennas Propag 45:316–328